

<sup>1</sup> The human visual system preserves the hierarchy  
<sup>2</sup> of 2-dimensional pattern regularity

<sup>3</sup> Peter J. Kohler<sup>1,2,3</sup> and Alasdair D. F. Clarke<sup>4</sup>

<sup>4</sup> *<sup>1</sup> York University, Department of Psychology, Toronto, ON M3J 1P3, Canada*

<sup>5</sup> *<sup>2</sup> Centre for Vision Research, York University, Toronto, ON, M3J 1P3, Canada*

<sup>6</sup> *<sup>3</sup> Stanford University, Department of Psychology, Stanford, CA 94305, United States*

<sup>7</sup> *<sup>4</sup> University of Essex, Department of Psychology, Colchester, UK, CO4 3SQ*

<sup>8</sup> **Abstract**

Symmetries are present at many scales in images of natural scenes. Humans and other animals are highly sensitive to visual symmetry, and a large literature has demonstrated contributions of symmetry to numerous domains of visual perception. The four fundamental symmetries, reflection, rotation, translation and glide reflection, can be combined in exactly 17 distinct ways. These *wallpaper groups* represent the complete set of symmetries in 2D images and have recently found use in the vision science community as an ideal stimulus set for studying the perception of symmetries in textures. The goal of the current study is to provide a more comprehensive description of responses to symmetry in the human visual system, by collecting both brain imaging (Steady-State Visual Evoked Potentials measured using high-density EEG) and behavioral (symmetry detection thresholds) data using the entire set of wallpaper groups. This allows us to probe the hierarchy of complexity among wallpaper groups, in which simpler groups are subgroups of more complex ones. We find that this hierarchy is preserved almost perfectly in both behavior and brain activity: A multi-level Bayesian GLM indicates that for most of the 63 subgroup relationships, subgroups produce lower amplitude responses in visual cortex (posterior probability: > 0.95 for 56 of 63) and require longer presentation durations to be reliably detected (posterior probability: > 0.95 for 48 of 63). This systematic pattern is seen only in visual cortex and only in components of the brain response known to be symmetric-specific. Our results show that representations of symmetries in the human brain are precise and rich in detail, and that this precision is reflected in behavior. These findings expand our understanding of symmetry perception, and open up new avenues for research on how fine-grained representations of regular textures contribute to natural vision.

Symmetries are abundant in natural and man-made environments, due to a complex interplay of physical forces that govern pattern formation in nature. Sensitivity to symmetry has been demonstrated in a number of species, includes bees (Giurfa et al., 1996), fish (Morris and Casey, 1998; Schlüter et al., 1998), birds (Møller, 1992; Swaddle and Cuthill, 1994) and dolphins (von Fersen et al., 1992), and may be used as a cue for mate selection in many species (Swaddle, 1999) including humans (Rhodes et al., 1998). Humans cultures have created and appreciated symmetrical patterns throughout history, and since the gestalt movement of the early 20th century, symmetry has been recognized as important for visual perception. Symmetry contributes

38 to the perception of shapes (Palmer, 1985; Li et al., 2013), scenes (Apthorp and Bell, 2015) and  
39 surface properties (Cohen and Zaidi, 2013). This literature is almost exclusively based on stimuli  
40 in which one or more symmetry axes are placed at a single point in the image. Focus has been  
41 on mirror symmetry or reflection, with relatively few studies including the other fundamental  
42 symmetries: rotation, translation and glide reflection (Wagemans, 1998) - perhaps because reflection  
43 has been found to be more perceptually salient (Mach, 1959; Royer, 1981; Palmer, 1991; Ogden  
44 et al., 2016; Hamada and Ishihara, 1988) and produce more brain activity (Makin et al., 2013, 2014,  
45 2012; Wright et al., 2015). In the current study, we take a different approach by investigating  
46 visual processing of regular textures in which combinations of the four fundamental symmetries  
47 tile the 2D plane.

48 In the two spatial dimensions relevant for images, symmetries can be combined in 17 distinct  
49 ways, the *wallpaper groups* (Fedorov, 1891; Polya, 1924; Liu et al., 2010). Previous work on a subset  
50 of four of the wallpaper groups used functional MRI to demonstrate that rotation symmetries  
51 in wallpapers elicit parametric responses in several areas in occipital cortex, beginning with  
52 visual area V3 (Kohler et al., 2016). This effect was also robust when symmetry responses were  
53 measured with electroencephalography (EEG) using both Steady-State Visual Evoked Potentials  
54 (SSVEPs)(Kohler et al., 2016) and Event-Related Potentials (Kohler et al., 2018). The SSVEP  
55 technique uses periodic visual stimulation to produce a periodic brain response that is confined to  
56 integer multiples of the stimulation frequency known as harmonics. SSVEP response harmonics  
57 can be isolated in the frequency domain and depending on the specific design, different harmonics  
58 will express different aspects of the brain response. (Norcia et al., 2015). Here we extend on the  
59 previous work by collecting SSVEPs and psychophysical data from human participants viewing  
60 the full set of wallpaper groups. We measure responses in visual cortex to 16 out of the 17  
61 wallpaper groups, with the 17th serving as a control stimulus. Our goal is to provide a more  
62 complete picture of how wallpaper groups are represented in the human visual system.

63 A wallpaper group is a topologically discrete group of isometries of the Euclidean plane, i.e.  
64 transformations that preserve distance (Liu et al., 2010). The wallpaper groups differ in the  
65 number and kind of these transformations and we can uniquely refer to different groups using  
66 crystallographic notation (CITATION?). In brief, most groups are notated by  $PXZ$ , where  $X \in \{1, 2, 3, 4, 6\}$  indicates the highest order of rotation symmetry and  $Z \in \{m, g\}$  indicates whether the  
67 pattern contains reflection (m) or glide reflection (g). For example,  $P4$  contains 4 fold rotation,  
68 while  $P2M$  contains 2 fold rotation and one reflection (see Figure XXX). Two of the groups start  
69 with a  $C$  rather than a  $P$ , ( $CM$  and  $CMM$ ) which indicates that the symmetries are specified relative  
70 to a cell that itself contains repetition. Full details of the naming convention and examples of the  
71 wallpaper groups can be found on wikipedia.

73 In mathematical group theory, when the elements of one group is completely contained in  
74 another, the inner group is called a subgroup of the outer group (Liu et al., 2010). The full list  
75 of subgroup relationships is listed in Section 1.4.2 of the Supplementary Material. Subgroup  
76 relationships between wallpaper groups can be distinguished by their indices. The index of a  
77 subgroup relationship is the number of cosets, i.e. the number of times the subgroup is found  
78 in the supergroup (Liu et al., 2010). As an example, let us consider groups  $P_2$  and  $P_6$  (see Figure

79 1C). If we ignore the translations in two directions that both groups share, group  $P_6$  consists of  
80 the set of rotations  $\{0^\circ, 60^\circ, 120^\circ, 180^\circ, 240^\circ, 300^\circ\}$ , in which  $P_2 \{0^\circ, 180^\circ\}$  is contained.  
81  $P_2$  is thus a subgroup of  $P_6$ , and  $P_6$  can be generated by combining  $P_2$  with rotations  $\{0^\circ, 120^\circ, 240^\circ\}$ .  
82 Because  $P_2$  is repeated three times in  $P_6$ ,  $P_2$  is a subgroup of  $P_6$  with index 3 (Liu et al., 2010). The  
83 17 wallpaper groups thus obey a hierarchy of complexity where simpler groups are subgroups of  
84 more complex ones (Coxeter and Moser, 1972).

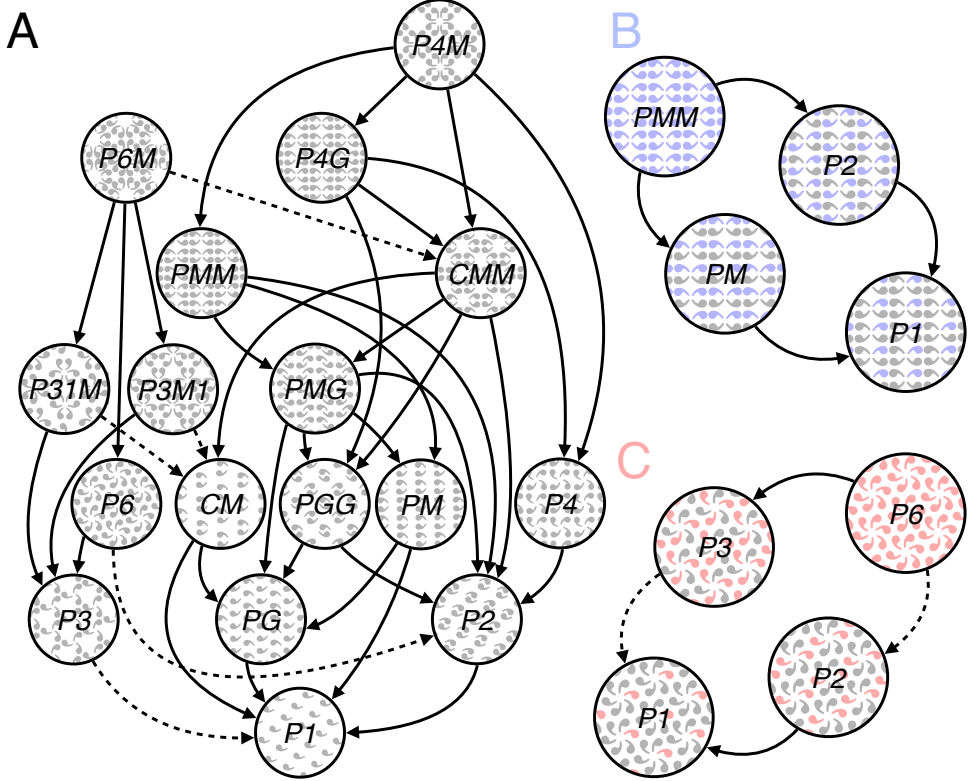


Figure 1: Subgroup relationships with indices 2 (solid lines) and 3 (dashed line) are shown in (A). All other relationships can be inferred by identifying the shortest path through the hierarchy, and multiplying the subgroup indices. For example,  $P_1$  is related to  $P_6$  through  $P_6 \rightarrow P_3$  (index 2) and  $P_3 \rightarrow P_1$  (index 3) so  $P_1$  is also a subgroup of  $P_6$  with index  $3 \times 2 = 6$ . We also show enlarged versions of some of the subgroup relationships involving  $PMM$  (B, shown in blue) and  $P_6$  (C, shown in red) and highlight the symmetries within the subgroups to emphasize how the supergroup can be generated by adding additional transformations to the subgroup.

85 The two datasets we present here make it possible to assess the extent to which both behavior  
86 and brain responses follow the hierarchy of complexity expressed by the subgroup relationships.  
87 Based on previous brain imaging work showing that patterns with more axes of symmetry pro-  
88 duce greater activity in visual cortex (Sasaki et al., 2005; Tyler et al., 2005; Kohler et al., 2018,  
89 2016; Keefe et al., 2018), we hypothesized that more complex groups would produce larger SSVEPs.  
90 For the psychophysical data, we hypothesized that more complex groups would lead to shorter  
91 symmetry detection thresholds, based on previous data showing that under a fixed presentation  
92 time, discriminability increases with the number of symmetry axes in the pattern (Wagemans  
93 et al., 1991). Our results confirm both hypotheses, and show that activity in human visual cortex  
94 is remarkably consistent with the hierarchical relationships between the wallpaper groups, with

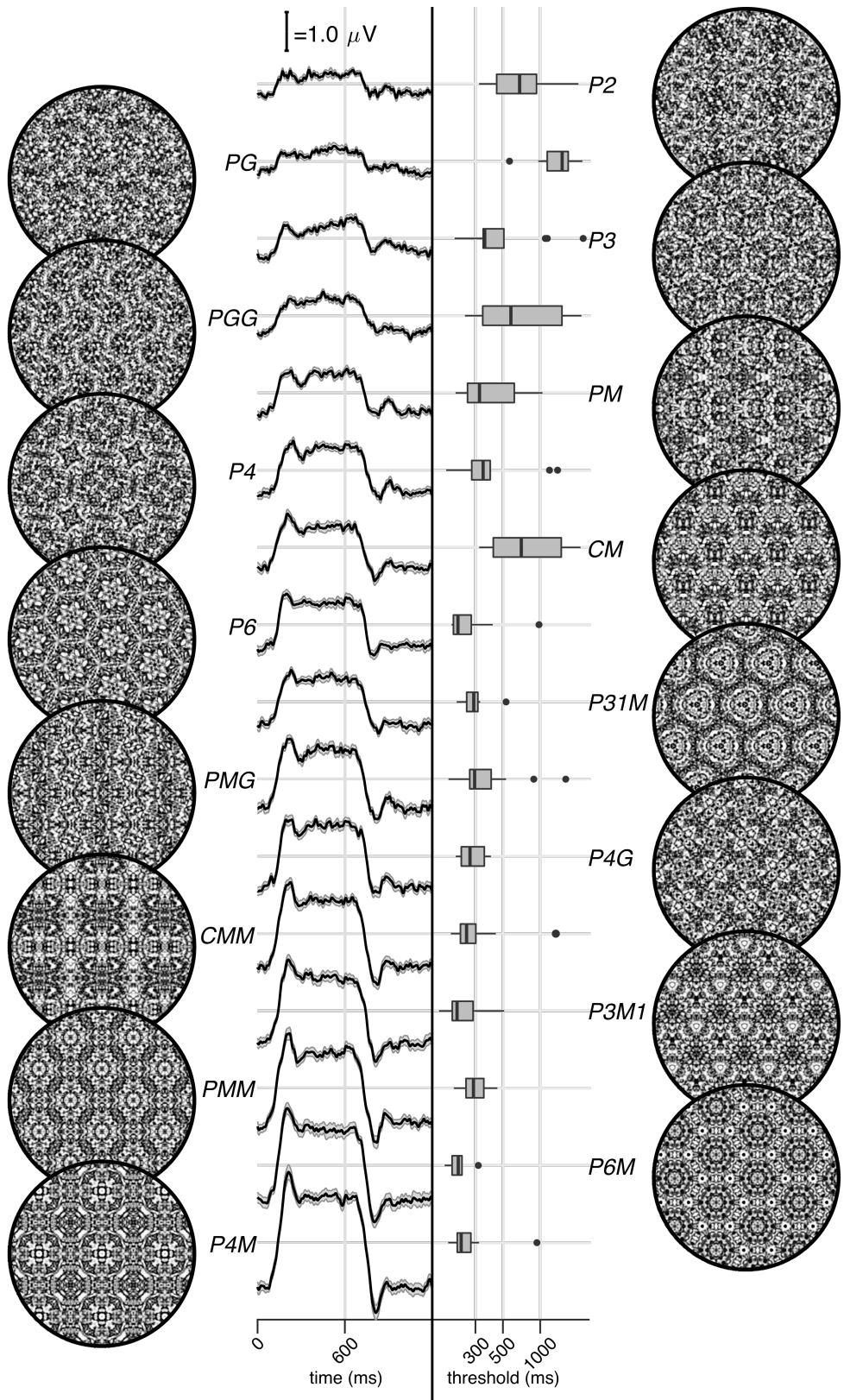


Figure 2: Examples of each of the 16 wallpaper groups are shown in the left- and right-most column of the figures, next to the corresponding SSVEP (center-left) and psychological (center-right) data from each group. The SSVEP data are odd-harmonic-filtered cycle-average waveforms. In each cycle, a  $P_1$  exemplar was shown for the first 600 ms, followed by the original exemplar for the last 600 ms. Errorbars are standard error of the mean. Psychophysical data are presented as boxplots reflecting the distribution of display duration thresholds. The 16 groups are ordered by the strength of the SSVEP response, to highlight the range of response amplitudes.

95 SSVEP amplitudes and psychophysical thresholds following these relationships at a level that is  
96 far beyond chance. The human visual system thus appears to encode all of the fundamental sym-  
97 metries using a representational structure that closely approximates the subgroup relationships  
98 from group theory.

## 99 Results

100 The stimuli used in our two experiments were generated from random-noise textures, which  
101 made it possible to generate multiple exemplars from each of the wallpaper groups, as described  
102 in detail elsewhere (Kohler et al., 2016). We generated control stimuli matched to each exemplar  
103 in the main stimulus set, by scrambling the phase but maintaining the power spectrum. All  
104 wallpaper groups are inherently periodic because of their repeating lattice structure. Phase  
105 scrambling maintains this periodicity, so the phase-scrambled control images all belong to group  
106  $P_1$  regardless of group membership of the original exemplar.  $P_1$  contains no symmetries other  
107 than translation, while all other groups contain translation in combination with one or more of the  
108 other three fundamental symmetries (reflection, rotation, glide reflection) (Liu et al., 2010). In our  
109 SSVEP experiment, this stimulus set allowed us to isolate brain activity specific to the symmetry  
110 structure in the exemplar images from activity associated with modulation of low-level features,  
111 by alternating exemplar images and control exemplars. In this design, responses to structural  
112 features beyond the shared power spectrum, including any symmetries other than translation,  
113 are isolated in the odd harmonics of the image update frequency (Kohler et al., 2016; Norcia et al.,  
114 2015, 2002). Thus, the combined magnitude of the odd harmonic response components can be  
115 used as a measure of the overall strength of the visual cortex response.

116 The psychophysical experiment took a distinct but related approach. In each trial an exemplar  
117 image was shown with its matched control, one image after the other, and the order varied pseudo-  
118 randomly such that in half the trials the original exemplar was shown first, and in the other half  
119 the control image was shown first. After each trial, participants were instructed to indicate  
120 whether the first or second image contained more structure. The duration of both images was  
121 controlled by a staircase procedure so that a threshold duration for symmetry detection could be  
122 computed for each wallpaper group.

123 Examples of the wallpaper groups and a summary of our brain imaging and psychophysical  
124 measurements are shown in Figure 2. For our primary SSVEP analysis, we only considered EEG  
125 data from a pre-determined region-of-interest (ROI) consisting of six electrodes over occipital cor-  
126 tex (see Supplementary Figure 1.1). SSVEP data from this ROI was filtered so that only the odd  
127 harmonics that capture the symmetry response contribute to the waveforms. While waveform am-  
128 plitude is quite variable among the 16 groups, all groups have a sustained negative-going response  
129 that begins at about the same time for all groups, 180 ms after the transition from the  $P_1$  control  
130 exemplar to the original exemplar. To reduce the amplitude of the symmetry-specific response to  
131 a single number that could be used in further analyses and compared to the psychophysical data,  
132 we computed the root-mean-square (RMS) over the odd-harmonic-filtered waveforms. The data  
133 in Figure 2 are shown in descending order according to RMS. The psychophysical results, shown

134 in box plots in Figure 2, were also quite variable between groups, and there seems to be a general  
135 pattern where wallpaper groups near the top of the figure, that have lower SSVEP amplitudes,  
136 also have longer psychophysical threshold durations.

137 We now wanted to test our two hypotheses about how SSVEP amplitudes and threshold du-  
138 rations would follow subgroup relationships, and thereby quantify the degree to which our two  
139 measurements were consistent with the group theoretical hierarchy of complexity. We tested  
140 each hypothesis using the same approach. We first fitted a Bayesian model with wallpaper group  
141 as a factor and participant as a random effect. We fit the model separately for SSVEP RMS and  
142 psychophysical data and then computed posterior distributions for the difference between su-  
143 pergroup and subgroup. These difference distributions allowed us to compute the conditional  
144 probability that the supergroup would produce (a) larger RMS and (b) a shorter threshold dura-  
145 tions, when compared to the subgroup. The posterior distributions are shown in Figure 3 for  
146 the SSVEP data, and in Figure 4 for the psychophysical data, which distributions color-coded  
147 according to conditional probability. For both data sets our hypothesis is confirmed: For the  
148 overwhelming majority of the 63 subgroup relationships, supergroups are more likely to produce  
149 larger symmetry-specific SSVEPs and shorter symmetry detection threshold durations, and in  
150 most cases the conditional probability of this happening is extremely high.

151 We also ran a control analysis using (1) odd-harmonic SSVEP data from a six-electrode ROI  
152 over parietal cortex (see Supplementary Figure 1.1) and (2) even-harmonic SSVEP data from the  
153 same occipital ROI that was used in our primary analysis. By comparing these two control  
154 analysis to our primary SSVEP analysis, we can address the specify of our effects in terms of  
155 location (occipital cortex vs parietal cortex) and harmonic (odd vs even). For both control analyses  
156 (plotted in Supplementary Figures 3.3 and 3.4), the correspondence between data and subgroup  
157 relationships was substantially weaker than in the primary analysis. We can quantify the strength  
158 of the association between the data and the subgroup relationships, by asking what proportion of  
159 subgroup relationships that reach or exceed a range of probability thresholds. This is plotted in  
160 Figure 5, for our psychophysical data, our primary SSVEP analysis and our two control SSVEP  
161 analyses. It shows that odd-harmonic SSVEP data from the occipital ROI and symmetry detection  
162 threshold durations both have a strong association with the subgroup relationships such that a  
163 clear majority of the subgroups survive even at the highest threshold we consider ( $p(\Delta > 0 | data) >$   
164 0.99). The association is far weaker for the two control analyses.

165 SSVEP data from four of the wallpaper groups ( $P_2$ ,  $P_3$ ,  $P_4$  and  $P_6$ ) was previously published  
166 as part of our earlier demonstration of parametric responses to rotation symmetry in wallpaper  
167 groups(Kohler et al., 2016). We replicate that result using our Bayesian approach, and find an  
168 analogous parametric effect in the psychophysical data (see Supplementary Figure 4.1). We also  
169 conducted an analysis testing for an effect of index in our two datasets and found that subgroup  
170 relationships with higher indices tended to produce greater pairwise differences between the  
171 subgroup and supergroup, for both SSVEP RMS and symmetry detection thresholds (see Supple-  
172 mentary Figure 4.2). The effect of index is relatively weak, but the fact that there is a measurable  
173 index effect can nonetheless be taken as preliminary evidence that representations of symmetries  
174 in wallpaper groups may be compositional.

Finally, we conducted a correlation analysis comparing SSVEP and psychophysical data and found a reliable correlation ( $R^2 = 0.44$ , Bayesian confidence interval [0.28, 0.55]). The correlation reflects an inverse relationship: For subgroup relationships where the supergroup produces a much *larger* SSVEP amplitude than the subgroup, the supergroup also tends to produce a much *smaller* symmetry detection threshold. This is consistent with our hypotheses about how the two measurements relate to symmetry representations in the brain, and suggests that our brain imaging and psychophysical measurements are at least to some extent tapping into the same underlying mechanisms.

## Discussion

Here we show that beyond merely responding to the elementary symmetry operations of reflection (Sasaki et al., 2005; Tyler et al., 2005) and rotation (Kohler et al., 2016), the visual system represents the hierarchical structure of the 17 wallpaper groups, and thus every *combination* of the four fundamental symmetries (rotation, reflection, translation, glide reflection) which comprise the set of regular textures. Both SSVEP amplitudes and symmetry detection thresholds preserve the hierarchy of complexity among the wallpaper groups that is captured by the subgroup relationships (Coxeter and Moser, 1972). For the SSVEP, this remarkable consistency was specific to the odd harmonics of the stimulus frequency that are known to capture the symmetry-specific response (Kohler et al., 2016) and to electrodes in a region-of-interest (ROI) over occipital cortex. When the same analysis was done using the odd harmonics from electrodes over parietal cortex (Supplementary Figure 3.3) or even harmonics from electrodes over occipital cortex (Supplementary Figure 3.4), the data was substantially less consistent with the subgroup relationships (yellow and green lines, Figure 5).

The current study uses 16 distinct wallpaper groups, while previous neuroimaging studies focused on a subset of 4 (Kohler et al., 2016, 2018). This represents a significant conceptual advance, because it makes it possible to investigate the complete subgroup hierarchy among the 17 groups and ask to what extent the hierarchy is reflected in brain activity. Our data provide a description of the visual system's response to the complete set of symmetries in the two-dimensional plane. We do not independently measure the response to  $P_1$ , but because each of the 16 other groups produce non-zero odd harmonic amplitudes (see Figure 2), we can conclude that the relationships between  $P_1$  and all other groups, where  $P_1$  is the subgroup, are also preserved by the visual system. The subgroup relationships are in many cases not obvious perceptually, and most participants had no knowledge of group theory. Thus, the visual system's ability to preserve the subgroup hierarchy does not depend on explicit knowledge of the relationships. Previous brain-imaging studies have found evidence of parametric responses with the number of reflection symmetry folds Keefe et al. (2018); Sasaki et al. (2005); Makin et al. (2016) and with the order of rotation symmetry Kohler et al. (2016). Our study is the first demonstration that the brain encodes symmetry in this parametric fashion across every possible combination of different *symmetry types*, and that this parametric encoding is also reflected in behavior. Previous behavioral experiments have shown that although naïve observers can distinguish many of the wallpaper groups (Landwehr, 2009),

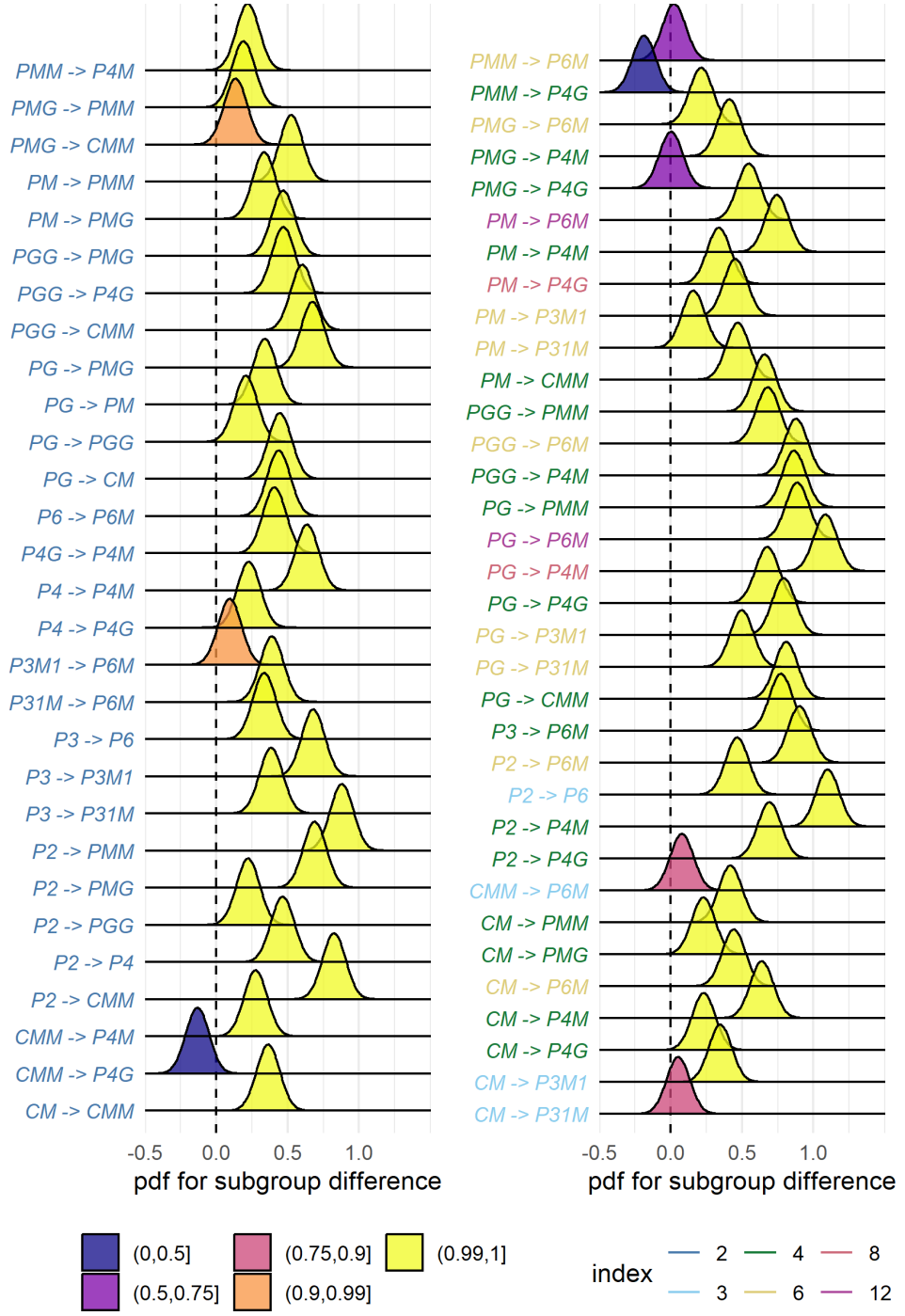


Figure 3: Posterior distributions for the difference in mean SSVEP RMS amplitude. Colour coding of the text indicates the index of the subgroup, while the colour of the filled distribution relates to the conditional probability that the difference in means is greater than zero. We can see that 55/63 subgroup relationships have  $p(\Delta|data) > 0.99$ .

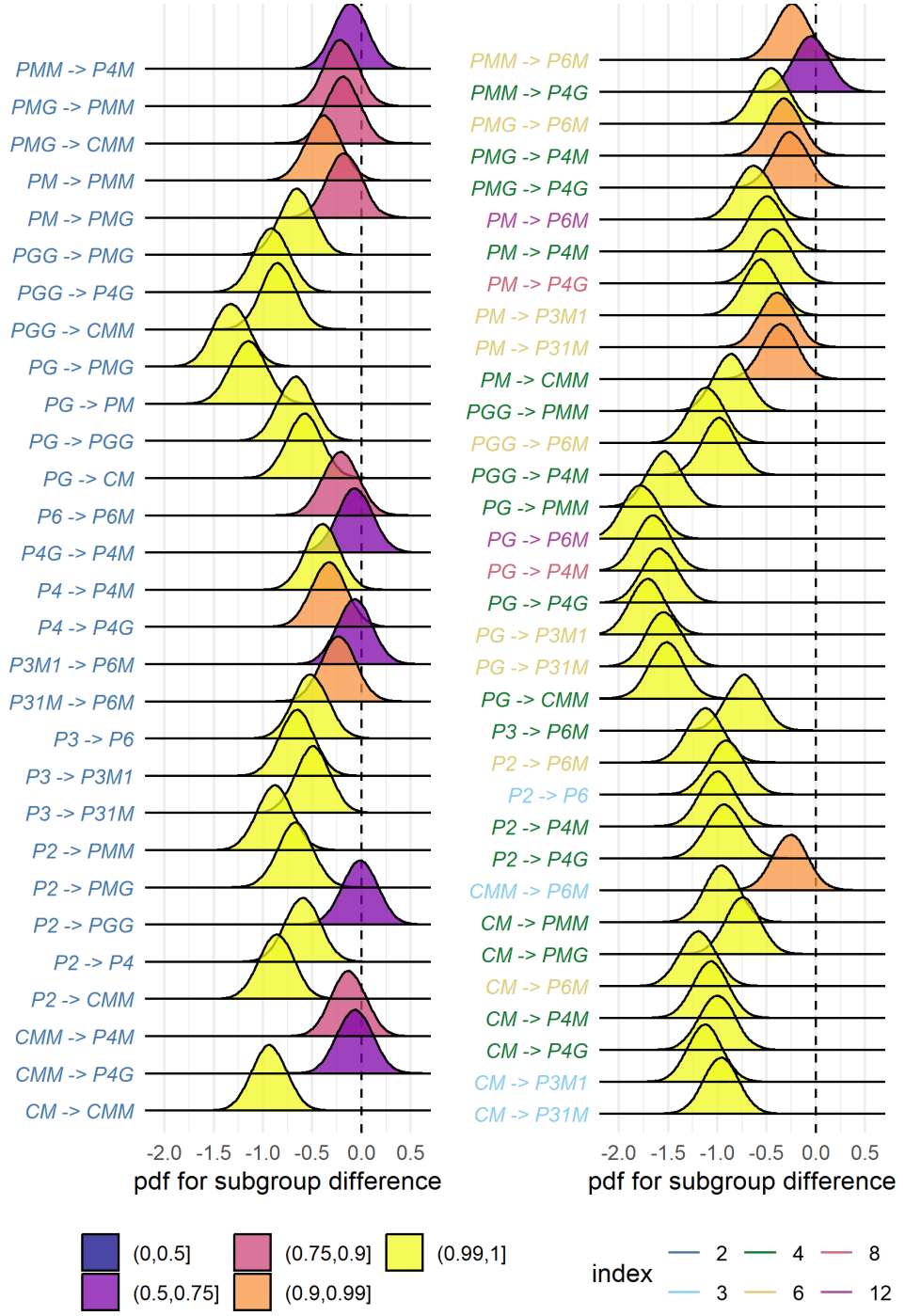


Figure 4: Posterior distributions for the difference in mean symmetry detection threshold durations. Colour coding of the text indicates the index of the subgroup, while the colour of the filled distribution relates to the conditional probability that the difference in means is greater than zero. We can see that 43/63 subgroup relationships have  $p(\Delta|data) > 0.99$ .

they tend to sort exemplars into fewer (4-12) sets than the number of wallpaper groups, often placing exemplars from different wallpaper groups in the same set (Clarke et al., 2011). The two-interval forced choice approach we use in the current psychophysical experiment makes it possible to directly compare symmetry detection thresholds to the subgroup hierarchy, and reveals that not only can the 17 wallpaper groups be distinguished based on behavioral data, behavior largely follows the subgroup hierarchy.

A large literature exists on the *Sustained Posterior Negativity* (SPN), a characteristic negative-going waveform that is known to reflect responses to symmetry and other forms of regularity and structure (Makin et al., 2016). The SPN scales with the proportion of reflection symmetry in displays that contain a mixture of symmetry and noise Makin et al. (2020); Palumbo et al. (2015), and both reflection, rotation and translation can produce a measurable SPN Makin et al. (2013). It has recently been demonstrated that a holographic model of regularity (van der Helm and Leeuwenberg, 1996), can predict both SPN amplitude (Makin et al., 2016) and perceptual discrimination performance (Nucci and Wagemans, 2007) for dot patterns that contain symmetry and other types of regularity. The available evidence suggests that the SPN and our SSVEP measurements are two distinct methods of isolating the same symmetry-related brain response: When observed in the time-domain, the symmetry-selective odd-harmonic responses produce similarly sustained waveforms (see Figure 2), odd-harmonic SSVEP responses can be measured for dot patterns similar to those used to measure the SPN (Norcia et al., 2002), and the one event-related study that has been published on the wallpaper groups produced SPN-like waveforms (Kohler et al., 2018). Future work should more firmly establish the connection and determine if the SPN can capture similarly precise symmetry responses as the SSVEPs presented here. It would also be worthwhile to ask if and how  $W$  can be computed for our random-noise based wallpaper textures where combinations of symmetries tile the plane.

We observe a reliable correlation between our brain imaging and psychophysical data. This suggests that the two measurements reflect the same underlying symmetry representations in visual cortex. It should be noted that the correlation is relatively modest ( $R^2 = 0.44$ ). This may be partly due to the fact that different individuals participated in the two experiments. It may also be related to the fact that participants were not doing a symmetry-related task during the SSVEP experiment, but instead monitored the stimuli for brief changes in contrast that occurred twice per trial (see Methods). Previous brain imaging studies have found enhanced reflection symmetry responses when participants performed a symmetry-related task (Makin et al., 2020; Sasaki et al., 2005; Keefe et al., 2018). It is possible that adding a symmetry-related task to our SSVEP experiment would have produced measurements that reflected subgroup relationships to an even higher extent than what we observed. On the other hand, our results are already close to ceiling (see Figure 5) and adding a symmetry-related task may simply enhance SSVEP amplitudes overall without improving the discriminability of individual groups, as has been observed for reflection by Keefe et al. (2018). Task-driven processing may be important for detecting symmetries that have been subject to perspective distortion, as suggested by SPN measurements (Makin et al., 2015) and somewhat less clearly in a subsequent functional MRI study (Keefe et al., 2018). Future work in which behavioral and brain imaging data are collected from the same participants,

255 and task is manipulated in the SSVEP experiment, will help further establish the connection be-  
256 tween the two measurements, and elucidate the potential contribution of task-related top-down  
257 processing to the current results.

258 We also find an effect of index for both our brain imaging measurements and our symmetry  
259 detection thresholds. This means that the visual system not only represents the hierarchical rela-  
260 tionship captured by individual subgroups, but also distinguishes between subgroups depending  
261 on how many times the subgroup is repeated in the supergroup, with more repetitions leading  
262 to larger pairwise differences. Our measured effect of index is relatively weak. This is perhaps  
263 because the index analysis does not take into account the *type* of isometries that differentiate the  
264 subgroup and supergroup. The effect of symmetry type can be observed by contrasting the mea-  
265 sured SSVEP amplitudes and detection thresholds for groups *PM* and *PG* in Figure 2. The two  
266 groups are comparable except *PM* contains reflection and *PG* contains glide reflection, and the  
267 former clearly elicits higher amplitudes and lower thresholds. An important goal for future work  
268 will be to map out how different symmetry types contribute to the representational hierarchy.

269 The correspondence between responses in the visual system and group theory that we demon-  
270 strate here, may reflect a form of implicit learning that depends on the structure of the natural  
271 world. The environment is itself constrained by physical forces underlying pattern formation  
272 and these forces are subject to multiple symmetry constraints (Hoyle, 2006). The ordered struc-  
273 ture of responses to wallpaper groups could be driven by a central tenet of neural coding, that of  
274 efficiency. If coding is to be efficient, neural resources should be distributed to capture the struc-  
275 ture of the environment with minimum redundancy considering the visual geometric optics, the  
276 capabilities of the subsequent neural coding stages and the behavioral goals of the organism (At-  
277 tneave, 1954; Barlow, 1961; Laughlin, 1981; Geisler et al., 2009). Early work within the efficient  
278 coding framework suggested that natural images had a  $1/f$  spectrum and that the corresponding  
279 redundancy between pixels in natural images could be coded efficiently with a sparse set of ori-  
280 ented filter responses, such as those present in the early visual pathway (Field, 1987; Olshausen  
281 and Field, 1997). Our results suggest that the principle of efficient coding extends to a much  
282 higher level of structural redundancy – that of symmetries in visual images.

283 The 17 wallpaper groups are completely regular, and relatively rare in the visual environment,  
284 especially when considering distortions due to perspective (see above) and occlusion. Near-regular  
285 textures, however, abound in the visual world, and can be modeled as deformed versions of the  
286 wallpaper groups (Liu et al., 2004). The correspondence between visual cortex responses and  
287 group theory demonstrated here may indicate that the visual system represents visual textures  
288 using a similar scheme, with the wallpaper groups serving as anchor points in representational  
289 space. This framework resembles norm-based encoding strategies that have been proposed for  
290 other stimulus classes, most notably faces (Leopold et al., 2006), and leads to the prediction that  
291 adaptation to wallpaper patterns should distort perception of near-regular textures, similar to  
292 the aftereffects found for faces (Webster and MacLin, 1999). Field biologists have demonstrated  
293 that animals respond more strongly to exaggerated versions of a learned stimulus, referred to  
294 as “supernormal” stimuli (Tinbergen, 1953). In the norm-based encoding framework, wallpaper  
295 groups can be considered *supertextures*, exaggerated examples of the near-regular textures com-

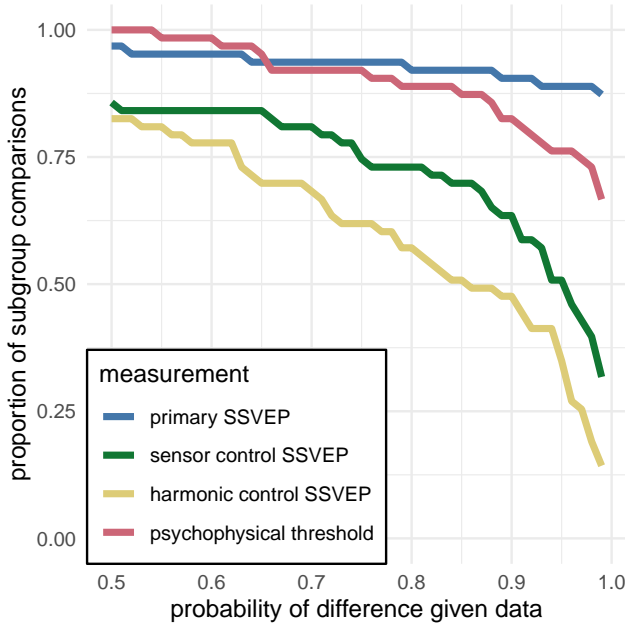


Figure 5: This plot shows the proportion of subgroup relationships that satisfy  $p(\Delta > 0 | data) > x$ . We can see that if we take  $x = 0.95$  as our threshold, the subgroup relationships are preserved in  $56/63 = 89\%$  and  $48/63 = 76\%$  of the comparisons for the primary SSVEP and threshold duration datasets, respectively. This compares to the  $32/63 = 51\%$  and  $22/63 = 35\%$  for the SSVEP control datasets.

mon in the natural world. If non-human animals employ a similar encoding strategy, they would be expected to be sensitive to symmetries in wallpaper groups. Recent functional MRI work in macaque monkeys offer some support for that: Macaque visual cortex responds parametrically to reflection and rotation symmetries in wallpaper groups, and the set of brain areas involved largely overlap those observed to be sensitive to symmetry in humans (Audurier et al., 2021). In human societies, visual artists may consciously or unconsciously create supernormal stimuli, to capture the essence of the subject and evoke strong responses in the audience (Ramachandran and Hirstein, 1999). Wallpaper groups are visually compelling, and symmetries have been widely used in human artistic expression going back to the Neolithic age (Jablan, 2014). If wallpapers are in fact supertextures, this prevalence may be a direct result of the strategy the human visual system has adopted for texture encoding.

## Participants

Twenty-five participants (11 females, mean age  $28.7 \pm 3.3$ ) took part in the EEG experiment. Their informed consent was obtained before the experiment under a protocol that was approved by the Institutional Review Board of Stanford University. 11 participants (8 females, mean age  $20.73 \pm 1.21$ ) took part in the psychophysics experiment. All participants had normal or corrected-to-normal vision. Their informed consent was obtained before the experiment under a protocol that was approved by the University of Essex's Ethics Committee. There was no overlap in participants between the EEG and psychophysics experiments.

315 **Stimulus Generation**

316 Exemplars from the different wallpaper groups were generated using a modified version of the  
317 methodology developed by Clarke and colleagues(Clarke et al., 2011) that we have described in de-  
318 tail elsewhere(Kohler et al., 2016). Briefly, exemplar patterns for each group were generated from  
319 random-noise textures, which were then repeated and transformed to cover the plane, according  
320 to the symmetry axes and geometric lattice specific to each group. The use of noise textures as  
321 the starting point for stimulus generation allowed the creation of an almost infinite number of  
322 distinct exemplars of each wallpaper group. To make individual exemplars as similar as possible  
323 we replaced the power spectrum of each exemplar with the median across exemplars within a  
324 group. We then generated control exemplars that had the same power spectrum as the exemplar  
325 images by randomizing the phase of each exemplar image. The phase scrambling eliminates ro-  
326 tation, reflection and glide-reflection symmetries within each exemplar, but the phase-scrambled  
327 images inherent the spectral periodicity arising from the periodic tiling. This means that all  
328 control exemplars, regardless of which wallpaper group they are derived from, are transformed  
329 into another symmetry group, namely  $P_1$ .  $P_1$  is the simplest of the wallpaper groups and contains  
330 only translations of a region whose shape derives from the lattice. Because the different wallpaper  
331 groups have different lattices,  $P_1$  controls matched to different groups have different power spectra.  
332 Our experimental design takes these differences into account by comparing the neural responses  
333 evoked by each wallpaper group to responses evoked by the matched control exemplars.

334 **Stimulus Presentation**

335 Stimulus Presentation. For the EEG experiment, the stimuli were shown on a 24.5" Sony Trimas-  
336 ter EL PVM-2541 organic light emitting diode (OLED) display at a screen resolution of  $1920 \times 1080$   
337 pixels, 8-bit color depth and a refresh rate of 60 Hz, viewed at a distance of 70 cm. The mean  
338 luminance was  $69.93 \text{ cd/m}^2$  and contrast was 95%. The diameter of the circular aperture in  
339 which the wallpaper pattern appeared was  $13.8^\circ$  of visual angle presented against a mean lumi-  
340 nance gray background. Stimulus presentation was controlled using in-house software. For the  
341 psychophysics experiment, the stimuli were shown on a  $48 \times 27 \text{ cm}$  VIEWPixx/3D LCD Display  
342 monitor, model VPX-VPX-2005C, resolution  $1920 \times 1080$  pixels, with a viewing distance of ap-  
343 proximately 40cm and linear gamma. Stimulus presentation was controlled using MatLab and  
344 Psychtoolbox-3 (Kleiner et al., 2007; Brainard, 1997). The diameter of the circular aperture for  
345 the stimuli was  $21.5^\circ$ .

346 **EEG Procedure**

347 Visual Evoked Potentials were measured using a steady-state design, in which  $P_1$  control images  
348 alternated with exemplar images from each of the 16 other wallpaper groups. Exemplar images  
349 were always preceded by their matched  $P_1$  control image. A single 0.83 Hz stimulus cycle consisted  
350 of a control  $P_1$  image followed by an exemplar image, each shown for 600 ms. A trial consisted of 10  
351 such cycles (12 sec) over which 10 different exemplar images and matched controls from the same  
352 rotation group were presented. For each group type, the individual exemplar images were always

353 shown in the same order within the trials. Participants initiated each trial with a button-press,  
354 which allowed them to take breaks between trials. Trials from a single wallpaper group were  
355 presented in blocks of four repetitions, which were themselves repeated twice per session, and  
356 shown in random order within each session. To control fixation, the participants were instructed  
357 to fixate a small white cross in the center of display. To control vigilance, a contrast dimming  
358 task was employed. Two times per trial, an image pair (*control P<sub>1</sub> plus exemplar*) was shown  
359 at reduced contrast. Participants were instructed to press a button on a response pad whenever  
360 they noticed a contrast change. Reaction times were not taken into account and participants were  
361 told to respond at their own pace while being as accurate as possible. We adjusted the reduction  
362 in contrast such that average accuracy for each participant was kept at 85% correct, in order to  
363 keep the difficulty of the vigilance task at a constant level.

### 364 Psychophysics Procedure

365 The experiment consisted of 16 blocks, one for each of the wallpaper groups (excluding *P<sub>1</sub>*). We  
366 used a two-interval forced choice approach. In each trial, participants were presented with two  
367 stimuli (one of which was the wallpaper group for the current block of trials, the other being *P<sub>1</sub>*),  
368 one after the other (inter-stimulus interval of 700ms). After each stimulus had been presented, it  
369 was masked with white noise for 300ms. After both stimuli had been presented, participants made  
370 a response on the keyboard to indicate whether they thought the first or second image contained  
371 more symmetry. Each block started with 10 practice trials, (stimulus display duration of 500ms)  
372 to allow participants to familiarise themselves with the current block's wallpaper pattern. If they  
373 achieved an accuracy of 9/10 in these trials they progressed to the rest of the block, otherwise  
374 they carried out another set of 10 practise trials. This process was repeated until the required  
375 accuracy of 9/10 was obtained. The rest of the block consisted of four interleaved staircases (using  
376 the QUEST algorithm (Watson and Pelli, 1983), full details given in the SI) of 30 trials each. On  
377 average, a block of trials took around 10 minutes to complete.

### 378 EEG Acquisition and Preprocessing

379 Steady-State Visual Evoked Potentials (SSVEPs) were collected with 128-sensor HydroCell Sensor  
380 Nets (Electrical Geodesics, Eugene, OR) and were band-pass filtered from 0.3 to 50 Hz. Raw data  
381 were evaluated off line according to a sample-by-sample thresholding procedure to remove noisy  
382 sensors that were replaced by the average of the six nearest spatial neighbors. On average, less  
383 than 5% of the electrodes were substituted; these electrodes were mainly located near the forehead  
384 or the ears. The substitutions can be expected to have a negligible impact on our results, as the  
385 majority of our signal can be expected to come from electrodes over occipital, temporal and parietal  
386 cortices. After this operation, the waveforms were re-referenced to the common average of all  
387 the sensors. The data from each 12s trial were segmented into five 2.4 s long epochs (i.e., each of  
388 these epochs was exactly 2 cycles of image modulation). Epochs for which a large percentage of  
389 data samples exceeding a noise threshold (depending on the participant and ranging between 25  
390 and 50  $\mu$ V) were excluded from the analysis on a sensor-by-sensor basis. This was typically the  
391 case for epochs containing artifacts, such as blinks or eye movements. Steady-state stimulation

will drive cortical responses at specific frequencies directly tied to the stimulus frequency. It is thus appropriate to quantify these responses in terms of both phase and amplitude. Therefore, a Fourier analysis was applied on every remaining epoch using a discrete Fourier transform with a rectangular window. The use of two-cycle long epochs (i.e., 2.4 s) was motivated by the need to have a relatively high resolution in the frequency domain,  $\delta f = 0.42$  Hz. For each frequency bin, the complex-valued Fourier coefficients were then averaged across all epochs within each trial. Each participant did two sessions of 8 trials per condition, which resulted in a total of 16 trials per condition.

## SSVEP Analysis

Response waveforms were generated for each group by selective filtering in the frequency domain. For each participant, the average Fourier coefficients from the two sessions were averaged over trials and sessions. The SSVEP paradigm we used allowed us to separate symmetry-related responses from non-specific contrast transient responses. Previous work has demonstrated that symmetry-related responses are predominantly found in the odd harmonics of the stimulus frequency, whereas the even harmonics consist mainly of responses unrelated to symmetry, that arise from the contrast change associated with the appearance of the second image (Norcia et al., 2002; Kohler et al., 2016). This functional distinction of the harmonics allowed us to generate a single-cycle waveform containing the response specific to symmetry, by filtering out the even harmonics in the spectral domain, and then back-transforming the remaining signal, consisting only of odd harmonics, into the time-domain. For our main analysis, we averaged the odd harmonic single-cycle waveforms within a six-electrode region of interest (ROI) over occipital cortex (electrodes 70, 74, 75, 81, 82, 83). These waveforms, averaged over participants, are shown in Figure 2. The same analysis was done for the even harmonics and for the odd harmonics within a six electrode ROI over parietal cortex (electrodes 53, 54, 61, 78, 79, 86; see Supplementary Figure 1.1). The root-mean square values of these waveforms, for each individual participant, were used to determine whether each of the wallpaper subgroup relationships were preserved in the brain data.

## Defining the list of subgroup relationships

In order to get the complete list of subgroup relationships, we digitized Table 4 from Coxeter (Coxeter and Moser, 1972) (shown in Supplementary Table 1.2). After removing identity relationships (i.e. each group is a subgroup of itself) and the three pairs of wallpaper groups that are subgroups of each other (e.g. *PM* is a subgroup of *CM*, and *CM* is a subgroup of *PM*) we were left with a total of 63 unambiguous subgroups that were included in our analysis.

## Bayesian Analysis of SSVEP and Psychophysical data

Bayesian analysis was carried out using R (v3.6.1) (R Core Team, 2019) with the *brms* package (v2.9.0) (Bürkner, 2017) and rStan (v2.19.2 (Stan Development Team, 2019)). The data from each experiment were modelled using a Bayesian generalised mixed effect model with wallpaper group

being treated as a 16-level factor, and random effects for participant. The SSVEP data and symmetry detection threshold durations were modelled using log-normal distributions with weakly informative,  $\mathcal{N}(0, 2)$ , priors. After fitting the model to the data, samples were drawn from the posterior distribution of the two datasets, for each wallpaper group. These samples were then recombined to calculate the distribution of differences for each of the 63 pairs of subgroup and supergroup. These distributions were then summarised by computing the conditional probability of obtaining a positive (negative) difference,  $p(\Delta|\text{data})$ . For further technical details, please see the [Supplementary Materials](#) where the full R code, model specification, prior and posterior predictive checks, and model diagnostics, can be found.

## References

- Apthorp, D. and Bell, J. (2015). Symmetry is less than meets the eye. *Current Biology*, 25(7):R267–R268.
- Attneave, F. (1954). Some informational aspects of visual perception. *Psychol Rev*, 61(3):183–93.
- Audurier, P., Héjja-Brichard, Y., Castro, V. D., Kohler, P. J., Norcia, A. M., Durand, J.-B., and Cottereau, B. R. (2021). Symmetry processing in the macaque visual cortex. *bioRxiv*, page 2021.03.13.435181. Publisher: Cold Spring Harbor Laboratory Section: New Results.
- Barlow, H. B. (1961). *Possible principles underlying the transformations of sensory messages*, pages 217–234. MIT Press.
- Brainard, D. H. (1997). Spatial vision. *The psychophysics toolbox*, 10:433–436.
- Bürkner, P.-C. (2017). Advanced bayesian multilevel modeling with the r package brms. *arXiv preprint arXiv:1705.11123*.
- Clarke, A. D. F., Green, P. R., Halley, F., and Chantler, M. J. (2011). Similar symmetries: The role of wallpaper groups in perceptual texture similarity. *Symmetry*, 3(4):246–264.
- Cohen, E. H. and Zaidi, Q. (2013). Symmetry in context: Salience of mirror symmetry in natural patterns. *Journal of vision*, 13(6).
- Coxeter, H. S. M. and Moser, W. O. J. (1972). *Generators and relations for discrete groups*. Ergebnisse der Mathematik und ihrer Grenzgebiete ; Bd. 148 Springer-Verlag, Berlin, New York.
- Fedorov, E. (1891). Symmetry in the plane. In *Zapiski Imperatorskogo S. Peterburgskogo Mineralogichesko Obshchestva [Proc. S. Peterb. Mineral. Soc.]*, volume 2, pages 345–390.
- Field, D. J. (1987). Relations between the statistics of natural images and the response properties of cortical cells. *J Opt Soc Am A*, 4(12):2379–94.
- Geisler, W. S., Najemnik, J., and Ing, A. D. (2009). Optimal stimulus encoders for natural tasks. *Journal of Vision*, 9(13):17–17.
- Giurfa, M., Eichmann, B., and Menzel, R. (1996). Symmetry perception in an insect. *Nature*, 382(6590):458–461. Number: 6590 Publisher: Nature Publishing Group.
- Hamada, J. and Ishihara, T. (1988). Complexity and goodness of dot patterns varying in symmetry. *Psychological Research*, 50(3):155–161.
- Hoyle, R. B. (2006). *Pattern formation: an introduction to methods*. Cambridge University Press.
- Jablan, S. V. (2014). *Symmetry, Ornament and Modularity*. World Scientific Publishing Co Pte Ltd, Singapore, SINGAPORE.
- Keefe, B. D., Gouws, A. D., Sheldon, A. A., Vernon, R. J. W., Lawrence, S. J. D., McKeefry, D. J., Wade, A. R., and Morland, A. B. (2018). Emergence of symmetry selectivity in the visual areas of the human brain: fMRI responses to symmetry presented in both frontoparallel and slanted planes. *Human Brain Mapping*, 39(10):3813–3826.
- Kleiner, M., Brainard, D., Pelli, D., Ingling, A., Murray, R., and Broussard, C. (2007). What's new in psychtoolbox-3. *Perception*, 36:1–16.

- 500 Kohler, P. J., Clarke, A., Yakovleva, A., Liu, Y., and Norcia, A. M. (2016). Representation of maximally regular textures in human visual cortex. *The Journal of Neuroscience*, 36(3):714–729. 545
- 501  
502  
503
- 504 Kohler, P. J., Cottreau, B. R., and Norcia, A. M. (2018). Dynamics of perceptual decisions about symmetry in visual cortex. *NeuroImage*, 167(Supplement C):316–330. 549 546
- 505  
506  
507
- 508 Landwehr, K. (2009). Camouflaged symmetry. *Perception*, 38:1712–1720. 550 551
- 509
- 510 Laughlin, S. (1981). A simple coding procedure enhances a neuron's information capacity. *Z Naturforsch C*, 36(9-10):910–2. 552 553 554
- 511  
512
- 513 Leopold, D. A., Bondar, I. V., and Giese, M. A. (2006). Norm-based face encoding by single neurons in the monkey inferotemporal cortex. *Nature*, 442(7102):572–5. 555 556
- 514  
515  
516
- 517 Li, Y., Sawada, T., Shi, Y., Steinman, R., and Pizlo, Z. (2013). *Symmetry Is the sine qua non of Shape*, book section 2, pages 21–40. Advances in Computer Vision and Pattern Recognition. Springer London. 560 561 562 563
- 518  
519  
520
- 521 Liu, Y., Hel-Or, H., Kaplan, C. S., and Van Gool, L. (2010). Computational symmetry in computer vision and computer graphics. *Foundations and Trends® in Computer Graphics and Vision*, 5(1–2):1–195. 564 565 566 567
- 522  
523  
524  
525
- 526 Liu, Y., Lin, W.-C., and Hays, J. (2004). Near-regular texture analysis and manipulation. In *ACM Transactions on Graphics (TOG)*, volume 23, pages 368–376. ACM. 568 569 570 571
- 527  
528  
529  
530  
531
- 532 Makin, A. D. J., Rampone, G., and Bertamini, M. (2015). Conditions for view invariance in the neural response to visual symmetry. *Psychophysiology*, 52(4):532–543. eprints 572 573
- 533  
534  
535  
536
- 537 Makin, A. D. J., Rampone, G., Morris, A., and Bertamini, M. (2020). The Formation of Symmetrical Gestalts Is Task-Independent, but Can Be Enhanced by Active Regularity Discrimination. *Journal of Cognitive Neuroscience*, 32(2):353–366. 584 585 586
- 538  
539  
540  
541
- Makin, A. D. J., Rampone, G., Pecchinenda, A., and Bertamini, M. (2013). Electrophysiological responses to visuospatial regularity. *Psychophysiology*, 50(10):1045–1055. eprint: <https://onlinelibrary.wiley.com/doi/pdf/10.1111/psyp.12082>. 547
- Makin, A. D. J., Rampone, G., Wright, A., Martinovic, J., and Bertamini, M. (2014). Visual symmetry in objects and gaps. *Journal of Vision*, 14(3):12–12. Publisher: The Association for Research in Vision and Ophthalmology. 550
- Makin, A. D. J., Wilton, M. M., Pecchinenda, A., and Bertamini, M. (2012). Symmetry perception and affective responses: A combined EEG/EMG study. *Neuropsychologia*, 50(14):3250–3261. 551
- Makin, A. D. J., Wright, D., Rampone, G., Palumbo, L., Guest, M., Sheehan, R., Cleaver, H., and Bertamini, M. (2016). An Electrophysiological Index of Perceptual Goodness. *Cerebral Cortex*, 26(12):4416–4434. 552
- Morris, M. R. and Casey, K. (1998). Female swordtail fish prefer symmetrical sexual signal. *Animal Behaviour*, 55(1):33–39. 553
- Møller, A. P. (1992). Female swallow preference for symmetrical male sexual ornaments. *Nature*, 357(6375):238–240. 554
- Norcia, A. M., Appelbaum, L. G., Ales, J. M., Cottreau, B. R., and Rossion, B. (2015). The steady-state visual evoked potential in vision research: A review. *Journal of Vision*, 15(6):4–4. 555
- Norcia, A. M., Candy, T. R., Pettet, M. W., Vildavski, V. Y., and Tyler, C. W. (2002). Temporal dynamics of the human response to symmetry. *Journal of Vision*, 2(2):132–139. 556
- Nucci, M. and Wagemans, J. (2007). Goodness of Regularity in Dot Patterns: Global Symmetry, Local Symmetry, and Their Interactions. *Perception*, 36(9):1305–1319. Publisher: SAGE Publications 557 558 559 560 561 562 563 564 565 566 567 568 569 570 571 572 573 574 575 576 577 578 579 580 581 582 583 584 585 586
- Ogden, R., Makin, A. D. J., Palumbo, L., and Bertamini, M. (2016). Symmetry Lasts Longer Than Random, but Only for Brief Presentations. *i-Perception*, 7(6):2041669516676824. Publisher: SAGE Publications. 587

- 585 Olshausen, B. A. and Field, D. J. (1997). Sparse coding with an overcomplete basis set: a strategy employed by v1? *Vision Res*, 37(23):3311–25.
- 588 Palmer, S. E. (1985). The role of symmetry in shape perception. *Acta Psychologica*, 59(1):67–90.
- 590 Palmer, S. E. (1991). Goodness, Gestalt, groups, and Garner: Local symmetry subgroups as a theory of figural goodness. In *The perception of structure: Essays in honor of Wendell R. Garner*, pages 23–39. American Psychological Association, Washington DC, US.
- 596 Palumbo, L., Bertamini, M., and Makin, A. (2015). Scaling of the extrastriate neural response to symmetry. *Vision Research*, 117:1–8.
- 599 Polya, G. (1924). Xii. Über die analogie der kristallsymmetrie in der ebene. *Zeitschrift für Kristallographie-Crystalline Materials*, 60(1):278–282.
- 602 R Core Team (2019). *R: A Language and Environment for Statistical Computing*. R Foundation for Statistical Computing, Vienna, Austria.
- 605 Ramachandran, V. S. and Hirstein, W. (1999). The science of art: A neurological theory of aesthetic experience. *Journal of Consciousness Studies*, 6(6–7):15–41.
- 609 Rhodes, G., Proffitt, F., Grady, J. M., and Sumich, A. (1998). Facial symmetry and the perception of beauty. *Psychonomic Bulletin & Review*, 5(4):651–669.
- 613 Royer, F. L. (1981). Detection of symmetry. *Journal of Experimental Psychology: Human Perception and Performance*, 7(6):1186–1210.
- 616 Sasaki, Y., Vanduffel, W., Knutson, T., Tyler, C., and Tootell, R. (2005). Symmetry activates extrastriate visual cortex in human and nonhuman primates. *Proceedings of the National Academy of Sciences of the United States of America*, 102(8):3159–3163.
- 621 Schlueter, A., Parzefall, J., and Schlupp, I. (1998). Female preference for symmetrical vertical bars in male sailfin mollies. *Animal Behaviour*, 56(1):147–153.
- 586 Stan Development Team (2019). RStan: the R interface to Stan. R package version 2.19.2.
- 589 Swaddle, J. P. (1999). Visual signalling by asymmetry: a review of perceptual processes. *Philosophical Transactions of the Royal Society of London. Series B: Biological Sciences*. Publisher: The Royal Society.
- 592 Swaddle, J. P. and Cuthill, I. C. (1994). Preference for symmetric males by female zebra finches. *Nature*, 367(6459):165–166. Number: 6459 Publisher: Nature Publishing Group.
- 594 Tinbergen, N. (1953). *The herring gull's world: a study of the social behaviour of birds*. Frederick A. Praeger, Inc., Oxford, England.
- 597 Tyler, C. W., Baseler, H. A., Kontsevich, L. L., Likova, L. T., Wade, A. R., and Wandell, B. A. (2005). Predominantly extra-retinotopic cortical response to pattern symmetry. *Neuroimage*, 24(2):306–314.
- 601 van der Helm, P. A. and Leeuwenberg, E. L. J. (1996). Goodness of visual regularities: A nontransformational approach. *Psychological Review*, 103(3):429–456. Publisher: American Psychological Association.
- 604 von Fersen, L., Manos, C. S., Goldowsky, B., and Roitblat, H. (1992). Dolphin Detection and Conceptualization of Symmetry. In Thomas, J. A., Kastelein, R. A., and Supin, A. Y., editors, *Marine Mammal Sensory Systems*, pages 753–762. Springer US, Boston, MA.
- 607 Wageman, J. (1998). Parallel visual processes in symmetry perception: Normality and pathology. *Documenta Ophthalmologica*, 95(3):359.
- 610 Wageman, J., Van Gool, L., and d'Ydewalle, G. (1991). Detection of symmetry in tachistoscopically presented dot patterns: effects of multiple axes and skewing. *Perception & Psychophysics*, 50(5):413–27.
- 613 Watson, A. B. and Pelli, D. G. (1983). Quest: A bayesian adaptive psychometric method. *Perception & Psychophysics*, 33(2):113–120.

- 665 Webster, M. A. and MacLin, O. H. (1999). Figure 666  
667 aftereffects in the perception of faces. *Psychon Bull*  
668 *Rev*, 6(4):647–53.
- (2015). Right-lateralized alpha desynchronization during regularity discrimination: Hemispheric specialization or directed spatial attention? *Psychophysiology*, 52(5):638–647. eprint: <https://onlinelibrary.wiley.com/doi/pdf/10.1111/psyp.12399>.